PPPL-1932

UC20-A,F

PPPL-1932

IMPURITY LEVELS AND POWER LOADING IN THE PDX TOKAMAK WITH HIGH POWER NEUTRAL BEAM INJECTION

By

R.J. Fonck, M. Bell, K. Bol, K. Brau, R. Budny, J.L. Cecchi, S. Cohen
S. Davis, H.F. Dylla, R. Goldston, B. Grek, R.J. Hawryluk, J. Hirschberg,
D. Johnson, R. Hulse, R. Kaita, S. Kaye, R.J. Knize, H. Kugel, D. Manos,
D. Mansfield, K. McGuire, D. Mueller, K. Oasa, M. Okabayashi, D.K. Owens,
J. Ramette, R. Reeves, M. Reusch, G. Schmidt, S. Sesnic, S. Suckewer,
H. Takahashi, F. Tenney, P. Thomas, M. Ulrickson, and R.V. Yelle

OCTOBER 1982

PLASMA PHYSICS LABORATORY

PRINCETON UNIVERSITY
PRINCETON, NEW JERSEY

PREPARED FOR THE U.S. DEPARTMENT OF ENERGY,
UNDER CONTRACT DE-AC02-76-CHO-3073.

NOTICE

Printed in the United States of America.

Available from:

National Technical Information Service
U. S. Department of Commerce
5285 Port Royal Road
Springfield, Virginia 22151

Price: Printed Copy $ * ; Microfische $3.50

*PAGES	NTIS Selling Price
1-25	$5.00
26-50	$6.50
51-75	$8.00
76-100	$9.50
101-125	$11.00
126-150	$12.50
151-175	$14.00
176-200	$15.50
201-225	$17.00
226-250	$18.50
251-275	$20.00
276-300	$21.50
301-325	$23.00
326-350	$24.50
351-375	$26.00
376-400	$27.50
401-425	$29.00
426-450	$30.50
451-475	$32.00
476-500	$33.50
500-525	$35.00
526-550	$36.50
551-575	$38.00
576-600	$39.50

For documents over 600 pages, add $1.50 for each additional 25 page increment.

PPPL--1932

DE83 001394

Impurity Levels and Power Loading in the PDX Tokamak with High Power Neutral Beam Injection*

R.J. Fonck, M. Bell, K. Bol, K. Brau, R. Budny, J.L. Cecchi, S. Cohen, S. Davis, H.F. Dylla, R. Goldston, B. Grek, R.J. Hawryluk, J. Hirschberg[1], D. Johnson, R. Hulse, R. Kaita, S. Kaye, R.J. Knize, H. Kugel, D. Manos, D. Mansfield, K. McGuire, D. Mueller, K. Oasa[2], M. Okabayashi, D.K. Owens, J. Ramette[3], R. Reeves, M. Reusch, G. Schmidt, S. Sesnic[4], S. Suckewer, H. Takahashi, F. Tenney, P. Thomas[5], M. Ulrickson, and R.V. Yelle

Princeton University, Plasma Physics Laboratory

Princeton, New Jersey 08544

Abstract

The PDX tokamak provides an experimental facility for the direct comparison of various impurity control techniques under reactor-like conditions. Four neutral beam lines can inject up to 6 MW for 300 ms. Carbon rail limiter discharges have been used to test the effectiveness of perpendicular injection, but non-disruptive full power operation for > 100 ms is difficult without extensive conditioning. Initial tests of a toroidal bumper limiter indicate reduced power loading and roughly similar impurity levels compared to the carbon rail limiter discharges. Poloidal divertor discharges with up to 5 MW of injected power are cleaner than similar circular discharges, and the power is deposited in a remote divertor chamber. High density divertor operation indicates a reduction of impurity flow velocity in the divertor and enhanced recycling in the divertor region during neutral injection.

*Presented at the 5th Intern. Conf. on Plasma Surface Interactions in Controlled Fusion Devices, Gatlinburg, May 1982.

[1] Physics Dept., University of Miami, Coral Gables, Florida.
[2] Japan Atomic Energy Research Institute, Tokai, Japan.
[3] Fontenay-aux-Roses, Euratom - CEA Association en Fusion, France.
[4] Institut für Plasma Physik, Garching, West Germany.
[5] JET-Joint Undertaking, Abingdon, United Kingdom.

I. Introduction

The Poloidal Divertor Experiment (PDX) tokamak provides a versatile facility for the direct comparison of a variety of impurity control methods which are relevant to the next generation of magnetic confinement devices, such as TFTR. As the thermal load on standard rail limiters has increased to levels of several kW/cm^2, it has become necessary to experimentally test a variety of impurity control techniques. Experiments such as PDX, D-III [1], ASDEX [2], and DITE [3] have been providing tests of a variety of divertor concepts, while tests of pumped limiter concepts [4] or extended toroidal limiters [5] are now also receiving increased attention. The toroidal bumper limiter in TFTR [6] is intended to absorb the plasma heat load and the direct neutral beam deposition on the inner wall due to incomplete absorption of the beam particles in the plasma. A test of a bumper limiter system under high power injection is thus highly desirable. A low-Z (graphite) rail limiter, a poloidal divertor, and a toroidal bumper limiter are all in use and a pumped limiter will soon be installed in PDX.

In the course of high power neutral beam heating experiments in PDX, data is being accumulated on the performance of several impurity control techniques under reactor-like power loading conditions. We report here the present status of the impurity levels in the main plasma and power loading levels on various limiting surfaces in PDX. In addition, some observations made on high density diverted plasmas with neutral beam injection indicate an approach to a high recycling divertor regime in PDX and are described here.

The PDX tokamak has been described in detail elsewhere [7], and only a few details are noted here. The major radius of the vacuum vessel is 145 cm, the maximum toroidal field is 24 kG, and the maximum plasma current is ~ 500 kA. A neutral beam injection (NBI) system (from the joint PPL-ORNL

Heating Project) can provide P_{inj} [illegible] 7.2 MW (50 keV, D°) for up to 150 ms or ~ 80% of full power for 300 ms. The four beam lines inject at a tangency radius of 35 cm, which gives an angle of 14° from perpendicular at the center of the vacuum vessel (R = 143 cm).

The modes of operation of PDX which are relevant to the present discussion are shown in Fig. 1. Figure 1(a) depicts a standard circular plasma configuration in which usually two graphite rail poloidal limiters (at the top and bottom of the discharge column) are used to isolate the plasma from the walls. These limiters are water cooled and can be moved remotely to vary the plasma minor radius from ~ 30 cm to ~ 50 cm. In this configuration, the plasma major radius can be varied from 135 to 155 cm. An alternate way to limit the plasma is depicted in Fig. 1(b), in which a toroidally symmetric bumper limiter is used to absorb the plasma load. It also provides a protective armor for the vacuum vessel from the neutral beams. The radius of the inside wall is 85 cm, giving a plasma major radius of 125 cm for a typical plasma minor radius of 40 cm. Finally, the poloidal divertor coils can be activated to divert the edge plasma to the remote neutralizer plates to reduce impurity recycling and provide a remote site for the plasma energy deposition. The standard Dee plasma, in which the plasma flows mainly into the inner set of neutralizer plates, Fig. 1(c), is obtained by moving the plasma to a major radius of 138 cm. Its minor radius is nominally 38 cm. Moving the discharge out to a major radius of 143 cm allows connection to both divertor regions in the 4-null configuration, Fig. 1(d). The neutralizer plates in the divertor region are made of titanium, as are the protective liners which shield the divertor coil hardware from the plasma.

Titanium gettering in the lower and upper divertor chambers provides a pumping speed of typically 2 x 10^5 ℓ/s for H_2. No gettering is done in the plasma main chamber. The vacuum vessel is conditioned by a combination of pulse discharge cleaning and glow discharge cleaning. The main intrinsic impurities are typically C, O, and Ti.

Plasma cleanliness has been monitored with a variety of diagnostics, including a bolometer array, absolutely calibrated vacuum ultraviolet spectrometers, an X-ray pulse height analyzer, and plasma resistivity estimates using the T_e profiles from Thomson scattering. Only the plasma resistivity data is available for comparison of all cases studied, and the other diagnostics mentioned above were used for supplemental information. All values of Z_{eff} quoted here are calculated from the resistivity using the Spitzer model. Energy deposition on limiting surfaces was monitored by using strategically placed thermocouples to measure bulk temperature changes. Where necessary, cooling models are used to estimate surface temperatures.

We note here that the Z_{eff} derived from a Spitzer resistivity model is expected to give an overestimate of the impurity content since trapping effects are not included. This is especially important for the beam heated plasmas with low collisionalities. For example, for a carbon rail limited plasma with P_{inj} = 3.2 MW, visible bremstrahlung measurements of Z_{eff} gave 1.8 during the ohmic phase and 3.4 during NBI while the resistivity Z_{eff} values were 1.8 and 4.1, respectively. However, the resistivity Z_{eff} quoted here is still useful for qualitative comparison of impurity levels in the various configurations described.

II. Graphite Rail Limiter Discharge

The main emphasis of the PDX program during 1981 was the investigation of the effectiveness of near-perpendicular neutral beam injection. The rail limiters were used most often in these studies to minimize uncertainties in operation and to take advantage of long experience with such systems, especially on PLT. Also, it was desired to compare heating efficiencies in PDX to those obtained in similar discharges in PLT to obtain a good evaluation of perpendicular injection. The results of these studies are reported in detail elsewhere [8] but we note here that heating efficiencies in PDX with perpendicular injection and PLT with tangential injection are comparable in similar discharges. In these discharges central ion temperatures of $\sim$ 6 keV were achieved with central $n_e \tau_E$ values up to $1.2 \times 10^{12} \mathrm{cm}^{-3}$ s (Fig. 2).

Radial profiles of radiated power were measured by a 19 channel bolometer array. Even in the presence of high power NBI, there are usually negligible amounts of radiated power loss from the center of the plasma. The radiation profiles are hollow, with central levels of $\lesssim$ 100 $\mathrm{mW/cm^3}$, as compared to central input powers of $\sim$ 1 $\mathrm{W/cm^3}$ or more. Volume integrated total radiated power account for $\sim$ 30% of the total input power (Fig. 3).

An estimate of power radiated by various impurities was made to verify the bolometer measurements. The absolute intensities of several spectral lines of Ti, O, and C were measured on the plasma midplane and compared to simple impurity transport models [9,10] to give estimates of total radiation levels from these impurities. The only centrally radiating impurity of consequence is Ti, whose concentration was measured to be $\sim 4 \times 10^{10}$ cm^{-3} with $P_{inj} \simeq 3$ MW and $n_e(0) \approx 4 \times 10^{13}$ cm^{-3}. The central emission from Ti is less than $\sim$ 50 $\mathrm{mW/cm^3}$, which is consistent with the low central radiation as seen by the bolometer. Bolometer and spectroscopy estimates of total radiated power agree in the absence of NBI, but with NBI the spectroscopic estimates can account for only $\sim$ 1/2 of the bolometer power levels. For the latter case, 50% of spectroscopically determined global radiated power was due to O, while Ti accounted for 40% and C the remaining 10%. The difference between the bolometer and spectroscopy results may be due to direct charge exchange loss of the beam particles.

Typical values of Z_{eff} range from $\sim$ 2 without NBI to $\sim$ 4 with high power injection. This rise in Z_{eff} cannot be accounted for by the observed Ti concentration, and presumably is due to an influx of C and O, whose edge radiation levels show large increases (e.g., OVI 1032Å emission increases by a factor of $\sim$ 4 above the ohmic heating level with $P_{inj} \simeq 6$ MW, while CIII 977Å emission shows a rise of $\sim$ 8). Measurements of O^{8+} and C^{6+} densities in the core of the discharge are in progress to verify that the rise in Z_{eff} is due to these low Z elements.

Preliminary analysis of the bulk temperature of the rail limiter as measured with thermocouples indicates that the limiters absorb about 15% of the total input power. Combining this with the bolometer results, $\sim$ 50% of the total input power remains unaccounted for. Presumably this can be explained by toroidally and poloidally asymmetric charge exchange losses and impurity radiation patterns with large enhancements in the vicinity of the limiter. Both the bolometer array and the VUV spectrometer are at least 90° toroidally away from the limiter position and hence are insensitive to enhanced signals near the limiter. With 4 neutral beams ($P_{inj} \gtrsim 6$ MW), peak power loads can reach 3 kW/cm^2 on the limiter. Bulk temperatures are typically 80-100°C. A nonlinear cooling model has been used to estimate a peak surface temperature of $\gtrsim$ 1600°C with highest beam powers. Usually a large influx of carbon is associated with such high surface temperatures. The discharges are often disruptive with all four beams ($P_{inj} \gtrsim 6$ MW) if the beam pulse length is $\gtrsim 150$ ms. During recent low q experiments, extensive operation (i.e., several weeks) with all four beams has apparently conditioned a single rail limiter well enough so that beam pulse lengths of 200 ms can be tolerated before disruption.

III. Bumper Limiter Discharges

Since the power handling capacity of the rail limiters seems to be reaching a limit without extensive conditioning, tests using the inner wall bumper limiter have recently been performed, and some initial results are reported here. The PDX inner wall bumper limiter has been described in detail by Kugel and Ulrickson [11]. This system, which acts as a prototype for the TFTR bumper limiter, consists of TiC coated graphite tiles (70% of total wall area) where the beams impinge on it. The rest of the wall is made of titanium tiles (Fig. 4), except for small breaks for diagnostic access (e.g., microwave horns, viewing dumps, etc.). The bumper limiter extends 30.5 cm above and below the vacuum vessel mid-plane, and its front face lies at a major radius of 85 cm, 13 cm from the vacuum vessel wall. Each TiC coated graphite tile is 9.9 cm wide, 12.2 cm high and 1.03 cm thick. The stainless steel backing plates with copper dovetail mounts for the tiles are water cooled to allow high duty cycles and for beam calorimetry.

The system has been tested as a beam protection plate by injection of a beam onto the TiC armor for 300 ms in the absence of a plasma ($P_{load} \simeq 3$ kW/cm^2). The bulk temperature of the wall rose to 350°C, while the instantaneous surface temperature was estimated to be 1800°C. No damage to the tiles occurred.

A noticeable feature of operating with the plasma in contact with the bumper limiter was that no special conditioning of the wall was needed, and non-disruptive discharges with $q(a) > 3$ were obtained immediately. The overall vacuum system was conditioned by ~ 4 weeks of high power operation with carbon limited discharges prior to operation on the bumper limiter. A few very fast disruptions have occurred with bumper limiter operation, but also several disruptions which were slower (in $\Delta I/\Delta t$) than the usual rail limiter case were also observed. Sufficient operating experience to obtain reasonable statistics on the nature of disruptions in these discharges is not yet available. Discharges with $q(a) \simeq 2$ have been achieved with the bumper limiter, but only fast disruptions (~ 100 kA/ms) occurred in this case. This points to the need for more tests with bumper limiter operation to characterize disruptive activity in such discharges before the next generation of tokamaks become operable.

One general difference between the rail and bumper limiters was that discharges with the bumper limiter required twice as much gas flow to fuel the discharge and hence it was harder to sustain the density than in the rail limiter case. This is described in more detail by Dylla et al. [13].

The impurity levels and radiated power estimates for these discharges are especially difficult to obtain because most diagnostic access in PDX provides a horizontal view into the vacuum vessel. Hence the bolometers, spectrometers and other diagnostics all view the active limiter and give unreliable global averages. Using a diagnostic neutral beam to actively probe the levels of O^{8+} and C^{6+} in the discharge center [12], and using standard VUV spectroscopy on highly ionized Ti gave $n_z/n_e \simeq 1\%$, 0.3%, and 0.02% for O,C, and Ti, respectively, in ohmically heated discharges. These levels were comparable to those obtained in rail limited discharges under similar operating conditions, but may be slightly inflated for O because of the presence of a small water leak in the armor cooling system prior to these measurements.

Detailed measurements of impurities or radiated power with high power NBI are not yet available, but measurements of Ti in the plasma core indicate levels comparable to rail limited discharges with NBI. For example, with $P_{inj} \simeq 3$ MW, $n_{Ti} \sim 2 \times 10^{10}$ cm^{-3} and can account for only 30 mW/cm^3 radiation at r = 0 (compared to an input of ~ 0.5 to 1 W/cm^3). Z_{eff} values are similar to those of NBI heated rail limited discharges, ranging from ~ 1.5 in the ohmic phase to 2.5 to 4 during NBI.

Typically 10 to 15% of the beam power is transmitted through the plasma to hit the armor directly. A toroidal average of total power incident on the bumper limiter (measured by an array of thermocouples around the machine) indicates that $P_{wall} \simeq 0.4\ P_{input}$. With a six minute shot cycle, the Ti sections reach a quasi-steady state bulk temperature of 50 to 100°C. The bulk temperature of the graphite tile beam armor sections are < 50°C for ohmic discharges and can rise to at least 50°C with high power injection. Typical load levels with $P_{inj} \sim 6$ MW are estimated to be ~ 0.2 kW/cm^2. The surface temperature is estimated to be $\lesssim$ 200°C. After two weeks of high power injection (P_{inj} = 2 to 5 MW), visual inspection through a viewport indicates that the TiC is intact and no damage is evident. The vertical power deposition profile is measured by a vertical thermocouple array behind a beam armor section. Figure 5 shows the change in bulk temperature per shot for an ohmic discharge. Similar profiles are obtained with NBI, but with the temperature change per shot being a few degrees higher. The minimum in this profile is reminiscent of the double peaked profile expected from the projection of the scrape-off plasma ($\lambda_{power} \sim$ few cm) onto the inner wall, as described by Schmidt [5]. The cause of the vertical asymmetry and displacement is not yet understood, but is observed to switch to the lower half if the toroidal field direction is reversed. For the data in Fig. 5, the ion drift direction was down, and the plasma current direction was such that the ions would hit the upper half of the bumper limiter.

IV. Divertor Discharges

A. Divertor Physics

The results of scrapeoff physics studies in the divertor discharges in PDX have been reported elsewhere and are only mentioned here. Probe measurements in the plasma midplane and in the divertor indicate that the density outside the separatrix of the D-shaped plasma falls off with a scale length of $\sim$ 5 cm and the electron temperature shows scale lengths of $\sim$ 7–10 cm with $T_e \simeq 8$ to 15 eV [15]. Recent results of studies of the plasma edge parallel power flow with a bolometer probe are reported by Manos et al. [16]. Typical scale lengths for the decay of parallel power flow are found to be $\lambda_p \sim 2.5$ cm for a Dee plasma measured several cm from separatrix, $\lambda_p \sim 1$ cm for a Dee plasma near the separatrix, $\lambda_p \sim 0.6$ cm for a 4-null plasma, and $\lambda_p \sim 2.5$ cm for a plasma with a carbon limiter.

The flow speed of impurities into the divertor was determined by measuring the relative Doppler shift of CII 4267Å radiation when viewing radially and tangentially along the edge of the neutralizer plate. The flow speed for CII in ohmically heated discharges was found to be comparable to the sound speed of the background plasma with $T_e \sim 15$ eV. Changing the working gas from H to D resulted in a reduction of v_{CII} by 1.4 [17].

B. Moderate Density Discharges with Neutral Injection

As reported by Bell et al. [17], recent operation with the divertor showed a random occurrence of large bursts of metallic influx, which were sometimes large enough to affect the plasma behavior. Spectroscopy observations found these impurities to be titanium and sometimes iron (possibly from the divertor coil can). The bursts were most troublesome when operating with a 4-null divertor, possibly arising from titanium deposited in the vacuum vessel dome or insufficient conditioning of the outer neutralizer plates. Running a Dee plasma and raising the position of the separatrix on the inner neutralizer plates markedly improved the situation and allowed reliable operation with high power injection. The observations reported here were made during $\sim$ 5 MW injection ($H^{\circ} \rightarrow D^{+}$) experiments to study plasma heating and density variations.

In general, the emissions of low Z impurities (O and C) are down by $\sim$ 1/2 from similar rail limiter plasmas during the ohmic phase. Also, the amount of Ti in the plasma core was similar to the circular plasma cases with ohmic heating. With NBI into moderate density ($\bar{n}_e \lesssim 4 \times 10^{13}$ cm^{-3}), Ti densities are similar to those reported above for the carbon rail limiters.

An example of the VUV spectrum from a neutral beam heated discharge is shown in Fig. 6. These data were obtained with an absolutely calibrated time-resolved multichannel spectrometer developed for PDX [18]. Of special interest is the fact that only the lower stages of ionization of C and O (e.g., CIII at 977Å and OII, OIII, at 833Å, OIV at 554Å) show large increases with the onset of NBI, while higher stages of ionization such as OV at 630Å and OVI at 1032Å, which presumably reside in annular shells somewhat inside the separatrix, show hardly any increase with NBI. The difference could be due to a changes in the edge plasma (e.g., higher n_e in the plasma scrape-off) or to enhanced recycling or shielding of impurities with NBI in the Dee plasmas. The increase in emission from highly ionized titanium is due to both the rise in $T_e(0)$, which results in more of the central Ti ionizing up to TiXIX and TiXX, and to rises in n_e and n_{Ti}.

The lack of a large rise in the OVI 1032Å or OV630Å emission with the onset of NBI suggests that the low-Z impurity influx into the plasma core may not be increasing significantly with NBI in contrast to observations with the rail limiters. This is borne out by the observation that Z_{eff} rises from 1.3 in the ohmic phase to only $\sim$ 1.7 with P_{inj} = 4.5 MW ($P_{absorbed} \simeq$ 3 MW). This value with NBI is consistently lower than that measured for the circular discharges. However, the bolometrically determined radiated power was $\sim$ 30 to 40% of the total input power absorbed, similar to the circular discharges. Efforts are underway to estimate how much of this can be due to beam particle charge exchange loss and will be reported elsewhere.

The energy handling characteristics of these Dee plasmas with $\bar{n}_e \sim 3 \times 10^{13}$ and $P_{inj} \sim$ 4.5 MW have also been studied. In addition to the 40% of the total input energy detected by the bolometers, the total energy incident on the neutralizer plates, measured by thermocouple arrays on the neutralizer plates, accounts for the remaining 60% of the absorbed energy, although experimental uncertainties can allow for $\sim$ 10% or so being unaccounted. The energy deposition profiles on the neutralizer plates with NBI are considerably more narrow than those with ohmic heating only. They are only a few cm wide and roughly peaked at the intersection of the separatrix with the neutralizer plates. The wider profiles obtained with ohmic heating only may be partly due to transient contributions to the total energy flux from the current build up and termination phases of the discharge. Peak power loads for these plasmas with NBI are $\sim$ 0.75 kW/cm^2, which is $\sim$ 1/4 of the peak load on the carbon limiter in circular discharges. Loads of up to 1 kW/cm^2 were sometimes recorded and some visual evidence of Ti sublimation was noted on the outer neutralizer plates after NBI into 2-null discharges.

An interesting observation during NBI into a Dee plasma is seen in Fig. 7, which shows the flow speed of CII along the field lines into the neutralizer plate before and during a 4.5 MW pulse of NBI. The flow speed essentially drops to zero during NBI. Even at only moderate plasma densities, apparently the plasma density and/or the neutral gas pressure near the neutralizers has built up enough to cause significantly increased recycling and reduction of bulk flow velocity along the field lines. The neutral gas pressure in the divertor dome far from the neutralizer plates was 2 x 10^{-4} Torr before NBI and rose to 4 x 10^{-4} Torr during NBI. Also shown in Fig. 7 is the > 3-fold increase in H_α emission in the divertor region and the much smaller increase in H_α emission on the main plasma midplane. This also points to a significant increase in recycling in the divertor region, even though the divertor geometry is still open [i.e., gas flow back to the main chamber is allowed through the unused outer divertor region Fig. 1(c)].

C. High Density Diverted Plasma with Neutral Beam Heating

Using the neutral beams to sustain the plasma and staggering the beam injection times allowed the attainment of discharges with $\bar{n}_e$ [illegible] 10^{14} cm^{-3} with full four beam injection ($H^\circ \rightarrow D^+$, P_{inj} = 4.5 MW) lasting for 150 ms. A number of noteworthy observations were made in these discharges.

As described by Dylla <u>et al.</u> [13] the Dee diverted discharges required a significant gas flow (typically $\sim$ 5 times more than the carbon limiter case) to fuel the discharge due to the reduced recycling of neutrals in the main chamber. The required gas load is increased even further with NBI and the flow of scrape-off plasma into the divertor domes and its subsequent neutralization results in neutral pressures in the divertor domes of $> 10^{-3}$ Torr even with the present open divertor geometry. This neutral pressure is on the order of that required to enter the medium neutral recycling regime defined by Post et al. [19], similar to the regime in which the D-III expanded boundary divertor plasmas operate [20]. A time evolution of the neutral pressure in the divertor dome for a high $\bar{n}_e$ PDX plasma is shown in Fig. 8.

As the density increases and the divertor neutral gas pressure builds up, the energy deposition profile on the neutralizer plate is found to broaden, and the peak power loading is subsequently reduced, as shown in Fig. 9. These profiles were obtained on the outer neutralizer plate of the inner divertor which absorbs > 90% of the total power incident on the divertor plates. In addition, with the increase in plasma density, the ratio of energy to the neutralizer plates to total absorbed energy reduces from 0.6 at $n_e \ell = 4 \times 10^{15}$ cm^{-2} to 0.5 at $n_e \ell \approx 8 \times 10^{15}$ cm^{-2}, while the fractional amount of radiated energy in the main plasma chamber remains a constant 0.4. A precipitous rise in H_α emission in the divertor region (enough to saturate the detector) also occurred during NBI on these high density discharges. Presumably, the energy that no longer is absorbed by the neutralizer plate is radiated or lost by charge exchange in the divertor region, but verification awaits further measurements.

The high density NBI discharges also showed very low values of Z_{eff}, $\lesssim 1.2$, during 4-beam injection. In addition, the central density of Ti was reduced by a factor of ~ 5 with respect to the lower $\bar{n}_e$ diverted plasma case, indicating a 10-fold reduction in central Ti concentration. Whether this reduction in n_{Ti} is due to significantly improved shielding of the plasma by the divertor scrape-off in the main chamber, reduced penetration of Ti from the divertor region to the main chamber, or the presence of a cold plasma causing reduced sputtering of Ti from the protective liners is unknown.

V. Discussion

A comparison of sample results obtained for each of the cases described above is given in Table I. In general, the divertor discharges have the lowest impurity levels with NBI, while the power loading on the limiting surface is lowest for the bumper limiter case. The divertor case is cleanest even though the limiting surfaces (i.e., the neutralizer plates) are made of titanium and the power load on this surface is comparable to that on the rail limiters in circular plasmas. Earlier studies have shown that the lower impurity levels in diverted discharges is usually due more to removal of the limiting surface to a region far from the main plasma than to shielding of impurities by the scrapeoff plasma. The fact that titanium densities in the divertor and graphite limited plasmas are similar indicates that very little of the Ti which is presumably released from the neutralizer plates actually reaches back to the main plasma. The residual Ti present in both rail limited and diverted discharges probably originates from the protective Ti liners which are in close proximity to the main plasma.

A summary of Z_{eff} data obtained during neutral beam power scans for each configuration discussed above is given in Fig. 10. These discharges are roughly similar in that the conditioning time for operation on each limiting surface was on the order of 2 to 4 weeks of non-disruptive operation of the machine with NBI at a wide variety of powers. The line average densities during NBI for the rail limiter, bumper limiter, and divertor discharges were 2 to 3 x 10^{13} cm^{-3}, 2 to 3 x 10^{13} cm^{-3}, and 4 x 10^{13} cm^{-3}, respectively. The safety factor at the plasma edge, $q(a)$, was > 2.5 for all three cases.

Overall, the diverted plasmas tend to have less impurity content during high power NBI than the other configurations for equivalent plasma parameters and similar conditioning periods, and it is easier to consistently produce clean plasmas with divertor operation.

We caution that these results do not mean that it is impossible to produce clean neutral beam heated discharges with the rail limiter. In contrast to the data in Fig. 10, very recent results during operation on a single rail limiter at $q(a) < 2$ (B_T [illegible] 10 kG) indicated that circular plasmas with $Z_{eff} < 2$ during NBI can be obtained after several weeks of operation at low q and high beam power. This indicates that the rail limiter can be conditioned over a long period to handle the power loads available in PDX. However, these low q discharges differ enough in power loads, limiters conditioning time, plasma profiles, edge plasma characteristics, MHD activity, and confinement properties that comparison with the results discussed here must be done with great caution. Power loading estimates and confirmation of plasma cleanliness for these low-q plasmas are not yet available, nor have similar discharges been studied yet with the divertors activated. Detailed studies of operation and impurity levels at low q(a) will be reported later.

Extension of these power loading and impurity control studies on PDX in the future will involve the application of a number of new diagnostics and some modifications to the machine itself. A time-resolved infrared TV camera [21] will be used to measure surface temperatures of the various limiting surfaces directly, which will reduce reliance on cooling model calculations. Since low-Z elements such as C and O are the major impurity species in PDX and other large tokamaks, use of diagnostics sensitive to their fully stripped ions is necessary. The use of charge exchange recombination techniques to measure O^{8+} and C^{6+} [12] and visible bremsstrahlung measures of Z_{eff} [22]

should allow the evaluation of central impurity levels and ionic composition in the presence of NBI.

In addition to rail limiters, bumper limiters, and divertors, pumped limiters and particle scoop limiters [4] are receiving attention as candidates for advanced impurity and particle control techniques in future tokamaks. It is thus desirable to study these approaches on PDX also to provide direct comparisons to other limiter concepts. Cecchi et al. have reported evidence of reduced recycling in ohmic discharges in PDX when ZrAl getter panels were placed near the PDX limiter [23]. Preliminary particle scoop measurements in the scrapeoff region of a divertor plasma in PDX were reported by Jacobsen [24]. A small particle scoop limiter (unpumped) was designed to allow the edge plasma flow to plug the entrance throat and thus reduce the return flow of neutralized gas to the discharge. Neutral gas pressures inside the scoop reached ~ 50 millitorr and showed a nonlinear increase with plasma density in the main chamber (Fig. 11).

Based on these encouraging results, a full-size scoop limiter has been fabricated for PDX and will be installed soon. Since no experimental results are available yet from this system, it is only briefly described here for completeness. A schematic view of the PDX pumped limiter is shown in Fig. 12. It is designed for operation with up to 6 MW of neutral injection power into the plasma and is estimated to be able to withstand 2 MW of power deposited on it for up to 300 ms. The surface of the copper neutralizer plate is coated with a 0.5 mm thick layer of vanadium to reduce sputtering. A pumping speed of ~ 4000 ℓ/s behind the limiter is achieved with a Ti getter ball. Diagnostics include a variety of pressure gauges, a residual gas analyzer, fixed and movable probes, calorimeters, and a shuttered viewport for an infrared camera or spectroscopy. A gas injection valve behind the limiter is also provided. Modelling calculations indicate that the scoop region of this limiter should scrapeoff ~ 10% of the edge particle flux and only a few percent of the total parallel energy flux.

Finally, the divertor hardware will be modified to achieve operation in the high recycling divertor regime even with ohmic discharges. The opening to the upper outer divertor region will be closed off to prevent the backflow of neutral gas from the divertor dome to the main plasma chamber, which should allow a buildup of a substantial pressure difference between the divertor region and main plasma. The aforementioned observations of high neutral gas pressure, stagnation of impurity flow, reduction in peak power loading on the neutralizer plates, and low Z_{eff} with NBI into divertor plasmas all indicate that operation in the medium to high recycling regime should allow the study of very clean plasmas with high injected powers in the near future.

VI. Conclusion

The PDX tokamak provides a facility for a direct comparison of all the major impurity and particle control and power handling technologies proposed for future tokamak facilities.

Although significant parameters have been achieved in tokamaks using graphite limiters, indications from PDX with 6 MW injection levels are that new impurity control and power loading techniques must be developed for the next generation of tokamak experiments. Carbon limiter circular plasmas in PDX have been used to achieve high T_i discharges and verify the effectiveness of perpendicular injection, but the low-Z impurity level (Z_{eff} ~ 3-4) with NBI is still unacceptable for future reactors. Initial tests of a toroidal bumper limiter with high power NBI have shown that the limiter works roughly as expected and no major problems or damage to the limiter have occurred, although the low-Z impurity levels with NBI are still significant. The occurrence of very fast disruptions in low q discharges with the bumper limiter must be investigated further. Further operation with the bumper limiters is also needed to determine if the low-Z impurity levels will decline with additional conditioning of the limiter surface. However, the low power loading on the bumper limiter suggests that long conditioning times may be necessary. Dee shaped diverted plasmas demonstrate consistently lower Z_{eff} than similar circular plasmas in the presence of NBI. Both the bumper limiter and divertor have peak power loads which are lower than those on the rail limiters. In addition, high density operation with 5 MW injection approaches conditions for high recycling divertor operation, as demonstrated by a stagnation of impurity flow velocity near the neutralizer plate, a large reduction in metallic impurity density in the plasma core, and large neutral gas pressures in the divertor dome even though the geometry is still open. Finally, tests of both a 6 MW capability scoop limiter and a high recycling divertor with closed geometry are planned for the near future.

Acknowledgments

This work was supported by the U.S. Department of Energy Contract NO. DE-AC02-76-CHO-3073. The authors thank the PDX technical crew and the entire PPPL support staff for assistance and support in these experiments.

REFERENCES

[1] M. Ali Mahdavi, in Proc. of Fifth Int. Conf. on Plasma Interactions in Controlled Surface, Fusion Devices, Gatlinburg, Tenn, May 3-7, 1982 (Paper E4); M. Shimada et al., same conference (Paper E5).

[2] W. Engelhardt and the ASDEX Team, in Proc. of Fifth Int. Conf. on Plasma Surface Interactions in Controlled Fusion Devices, Gatlinburg, Tenn, May 3-7, 1982 (Paper E2).

[3] P.C. Johnson, in Proc. of Fifth Int. Conf. on Plasma Surface Interactions in Controlled Fusion Devices, Gatlinburg, Tenn, May 3-7, 1982 (Paper E1).

[4] P. Mioduszewski, in Proc. of Fifth Int. Conf. on Plasma Surface Interactions in Controlled Fusion Devices, Gatlinburg, Tenn, May 3-7 1982 (Paper C1).

[5] J.A. Schmidt, Comm. on Plasma Phys. and Controlled Fusion V (1980) 225.

[6] J.L. Cecchi, Nucl. Mater. 93 & 94 (1980) 28.

[7] D.M. Meade et al., in Proc. Eighth Int. Conf. on Plasma Physics and Controlled Nuclear Fusion Research (IAEA, Vienna, 1981) Vol. 1, p. 665.

[8] R.J. Hawryluk et al., Phys. Rev. Lett. 49 (1982) 326.

[9] R.C. Isler and E.C. Crume, Nucl. Fusion 6 (1979) 727.

[10] R.J. Hawryluk, S. Suckewer, and S.P. Hirschman, Nucl. Fusion 5 (1979) 607.

[11] H.W. Kugel, M. Ulrickson, Princeton University, Plasma Physics Laboratory Report PPPL-1785 (August 1981) 27; to be published in Nuclear Technology (1982).

[12] R.J. Fonck et al., Phys. Rev. Lett. 49 (1982) 737.

[13] H.F. Dylla et al., in Proc. of Fifth Int. Conf. on Plasma Surface Interactions in Controlled Fusion Devices, Gatlinburg, Tenn, May 3-7, 1982 (Paper B5).

[14] D.K. Owens et al., Nucl. Mater. 93 & 94 (1980) 213.

[15] R. Budny, Princeton University, Plasma Physics Laboratory Report PPPL-1876 (Feb. 1982) 15.

[16] D. Manos et al., in Proc. of Fifth Int. Conf. on Plasma Surface Interactions in Controlled Fusion Devices, Gatlinburg, Tenn, May 3-7, 1982 (Paper A10).

[17] M.G. Bell et al., Recent PDX Results, in Proceedings of X European Conference on Controlled Fusion and Plasma Physics Moscow, USSR, September 14-19, 1981.

[18] R.J. Fonck, A.T. Ramsey, and R.V. Yelle, Applied Optics 21 (1982) 2115.

[19] D.E. Post, M. Petravic, and D. Heifetz, in Proc. of Fifth Int. Conf. on Plasma Surface Interactions in Controlled Fusion Devices, Gatlinburg, Tenn, May 3-7, 1982 (Paper D1).

[20] M. Ali Mahdavi et al., Phys. Rev. Lett. 47 (1981) 1602.

[21] R.A. Jacobsen, Princeton University, Plasma Physics Laboratory Report PPPL-1826 (August 1981) 19.

[22] K. Kadota, M. Otsuka, and F. Fujita, Nucl. Fusion 20 (1980) 209.

[23] J.L. Cecchi et al., in Proc. of Fifth Int. Conf. on Plasma Surface Interactions in Controlled Fusion Devices, Gatlinburg, Tenn, May 3-7, 1982 (Paper C9).

[24] R.A. Jacobsen, Nucl. Fusion 22 (1982) 27.

Table I. Power Loading in PDX Discharges With Neutral Beam Heating

	Graphite Rail (9/23/81)	Bumper Limiter (3/19/82)	Divertor (8/14/81)
Beam Species	$D^\circ \to H^+$	$D^\circ \to H^+$	$H^\circ \to D^+$
$\Delta t_{(Beam)}$ (msec)	150	150	150
P_{inj} (MW)	4.4	4.1	4.5
$P_{absorbed}$ (MW)	3.4	3.2	3.6
P_{OH} (MW)	0.2	0.3	0.2
$\bar{n}_e$ (cm^{-3})	2.5×10^{13}	2.5×10^{13}	4.3×10^{13}
Limiting Surface Material	C	TiC/C (70%) T_i (30%)	Ti
$\frac{E_{Limiting\ Surface}}{E_{IN}}$	0.19	0.49	0.60
P_{Load} (kW/cm^2)	1.9	0.2	0.75
Z_{eff}(OH-NBI) (Spitzer)	2.0-4.5	1.8-2.9	1.3-1.7
$\frac{P_{Bolometer}}{P_{IN}}$	0.30	N/A	0.40

Figure Captions

Fig. 1 Modes of operation in PDX. a) Graphite rail limiter. R = 135 to 155 cm. b) Inner wall bumper limiter. R = 125 cm. c) D-shaped or Dee diverted plasma. R = 138 cm. d) Four-null or square diverted plasma. R = 143 cm.

Fig. 2 Ion temperatures in PDX with high power injection and graphite rail limiters.

Fig. 3 Total power radiated from PDX plasma as a function of neutral beam power. These measurements are from circular discharges with graphite rail limiters. = Bolometer; 0 = VUV Spectroscopy. The inset shows radiation profiles as measured by the bolometer array.

Fig. 4 Schematic top view of PDX showing the locations of the coated graphite and titanium inner wall bumper limiter. Also shown are the location and injection angles of the PDX neutral beam injection system.

Fig. 5 Bulk temperature change per discharge in bumper limiter for ohmic discharges.

Fig. 6 VUV spectra from a single PDX discharge with neutral beam injection from t = 400 to 550 ms.

Fig. 7 Reduction of impurity flow velocity in the divertor region with NBI. Also shown is the H_α emission from the divertor region and the main plasma midplane.

Fig. 8 Time evolution of neutral gas pressure in the divertor dome with high n_e and ~ 4.5 MW. The pressure gauge saturated at 7×10^{-4} Torr.

Fig. 9 Energy deposition profile into Dee divertor as a function plasma density. Position denotes height above bottom of neutralizer plate. P_{inj} = 4.5 MW.

Fig. 10 Z_{eff} from Thomson scattering data for neutral beam heated PDX plasmas operating with graphite rail limiters ($D^\circ \to H^+$), the inner wall bumper limiter ($D^\circ \to H^+$), or the Dee shaped divertor ($H^\circ \to D^+$). Spitzer resistivity is assumed for all cases.

Fig. 11 Variation in neutral gas pressure in particle scoop in the plasma scrape-off region of a Dee shaped plasma. $\int n d\ell$ is measured along the plasma midplane.

Fig. 12 Schematic of details of the PDX Particle Scoop limiter designed for operation with 6 MW of injected power. a) Overall system. b) Midplane cross section.

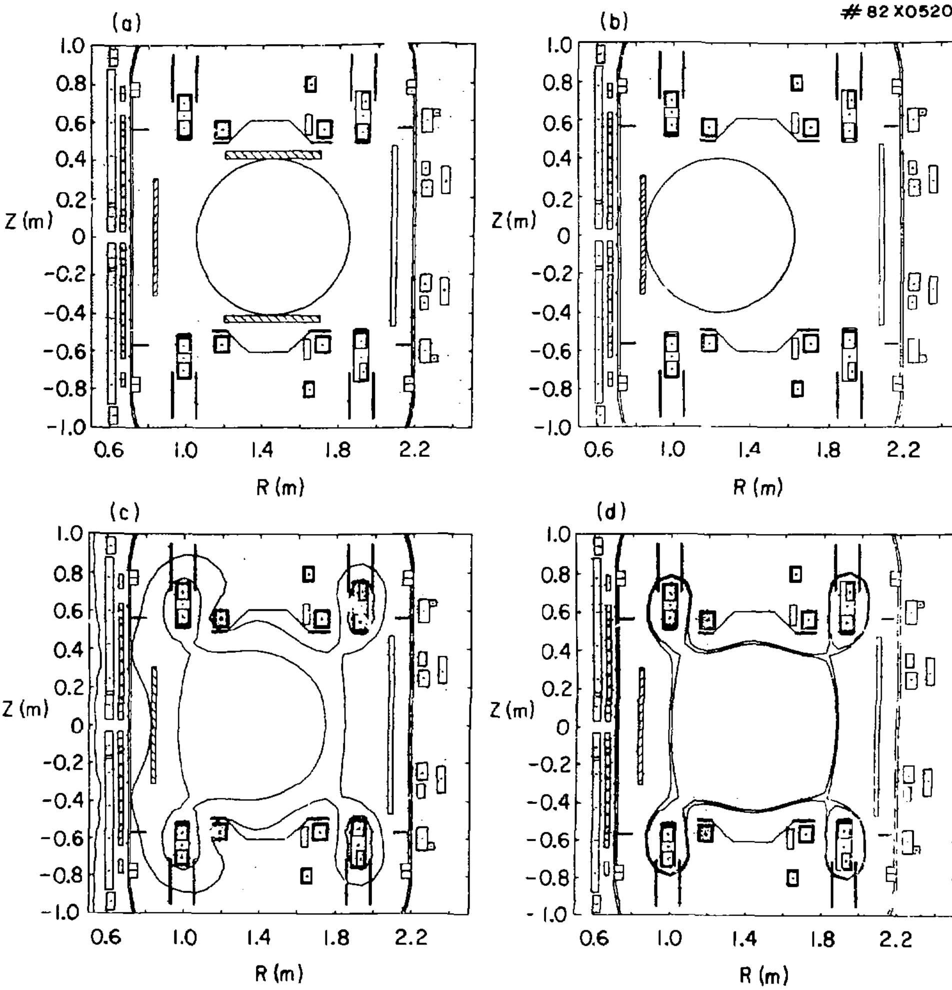

Fig. 1

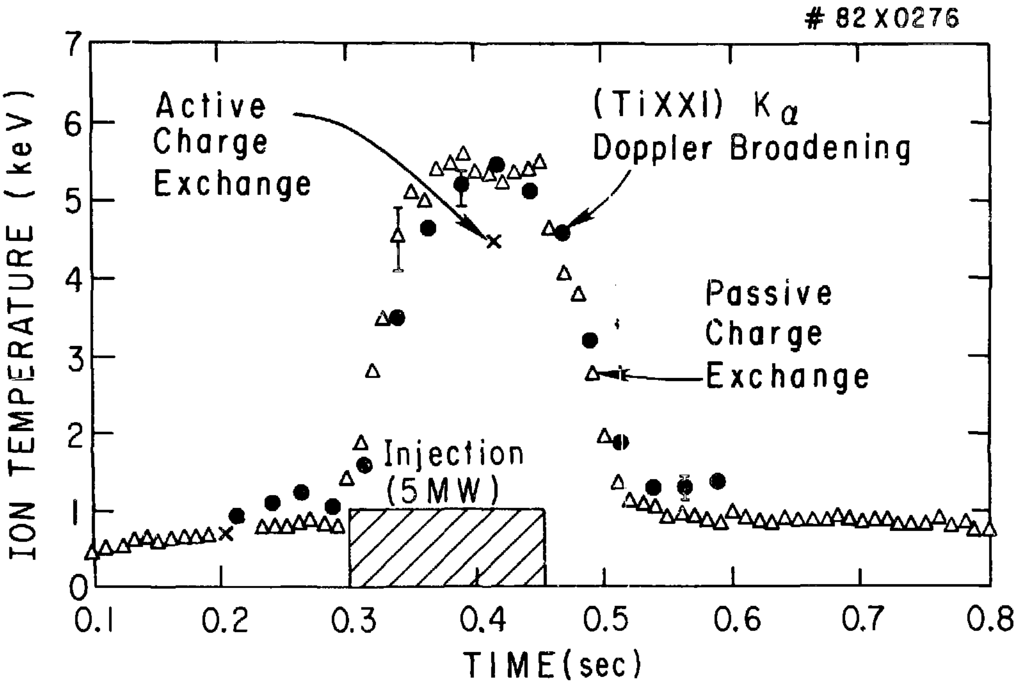

82X0276
ION TEMPERATURE (keV)
Active
Charge
Exchange
(TiXXI) Kα
Doppler Broadening
Passive
Charge
Exchange
Injection
(5MW)
TIME(sec)
0
1
2
3
4
5
6
7
0.1
0.2
0.3
0.4
0.5
0.6
0.7
0.8

Fig. 2

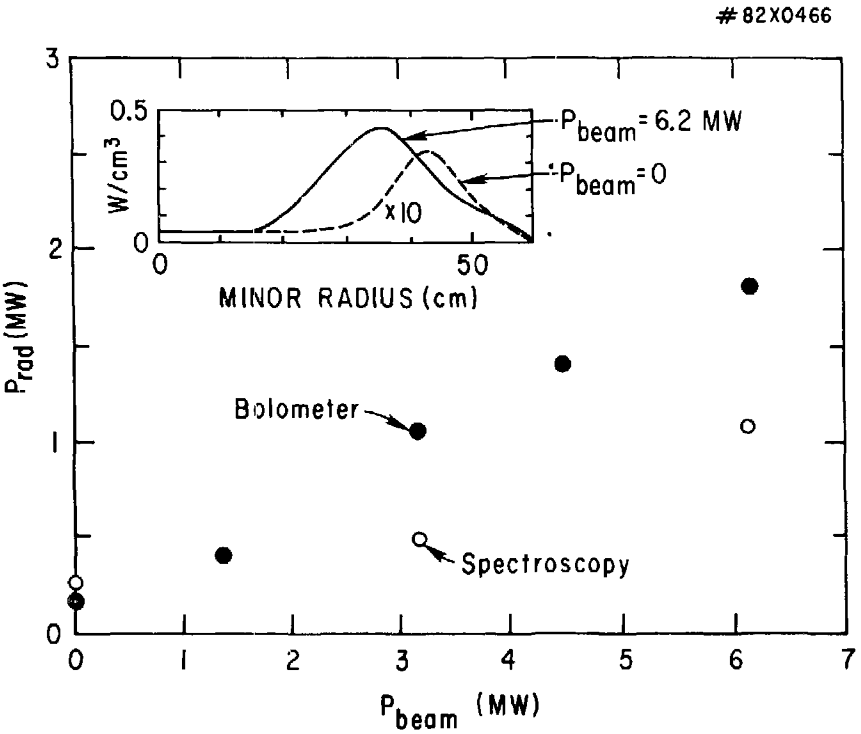

#82X0466
0.5
W/cm3
0
0
50
MINOR RADIUS (cm)
Pbeam = 6.2 MW
Pbeam = 0
x10
3
2
1
0
Prad (MW)
Bolometer
Spectroscopy
0
1
2
3
4
5
6
7
Pbeam (MW)

Fig. 3

PDX INSTALLATION, PARTIAL TOP VIEW

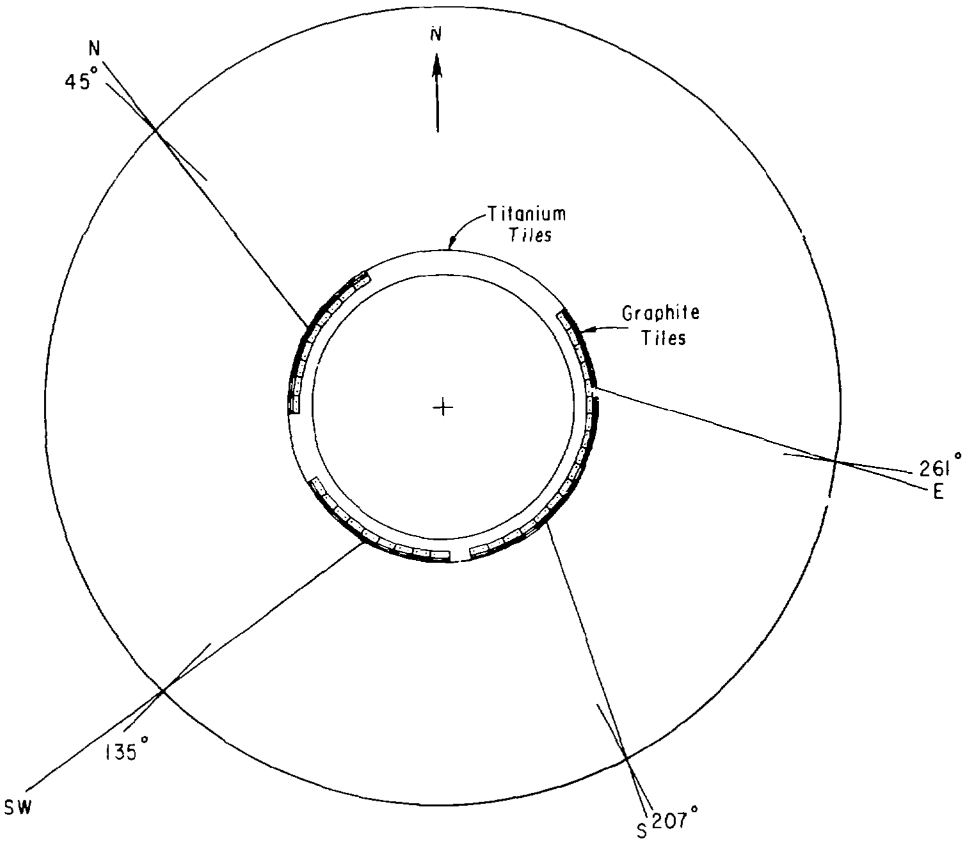

Fig. 4

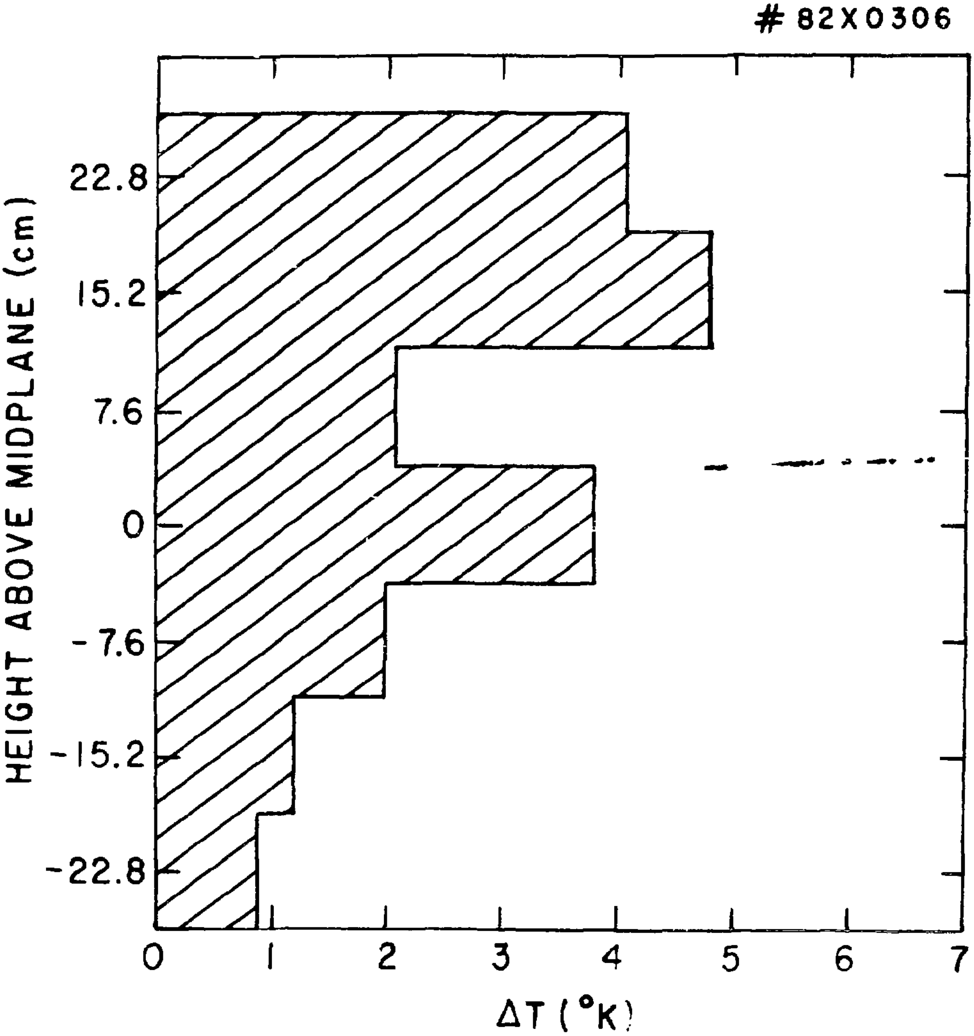

82X0306
HEIGHT ABOVE MIDPLANE (cm)
22.8
15.2
7.6
0
-7.6
-15.2
-22.8
0
1
2
3
4
5
6
7
ΔT (°K)

Fig. 5

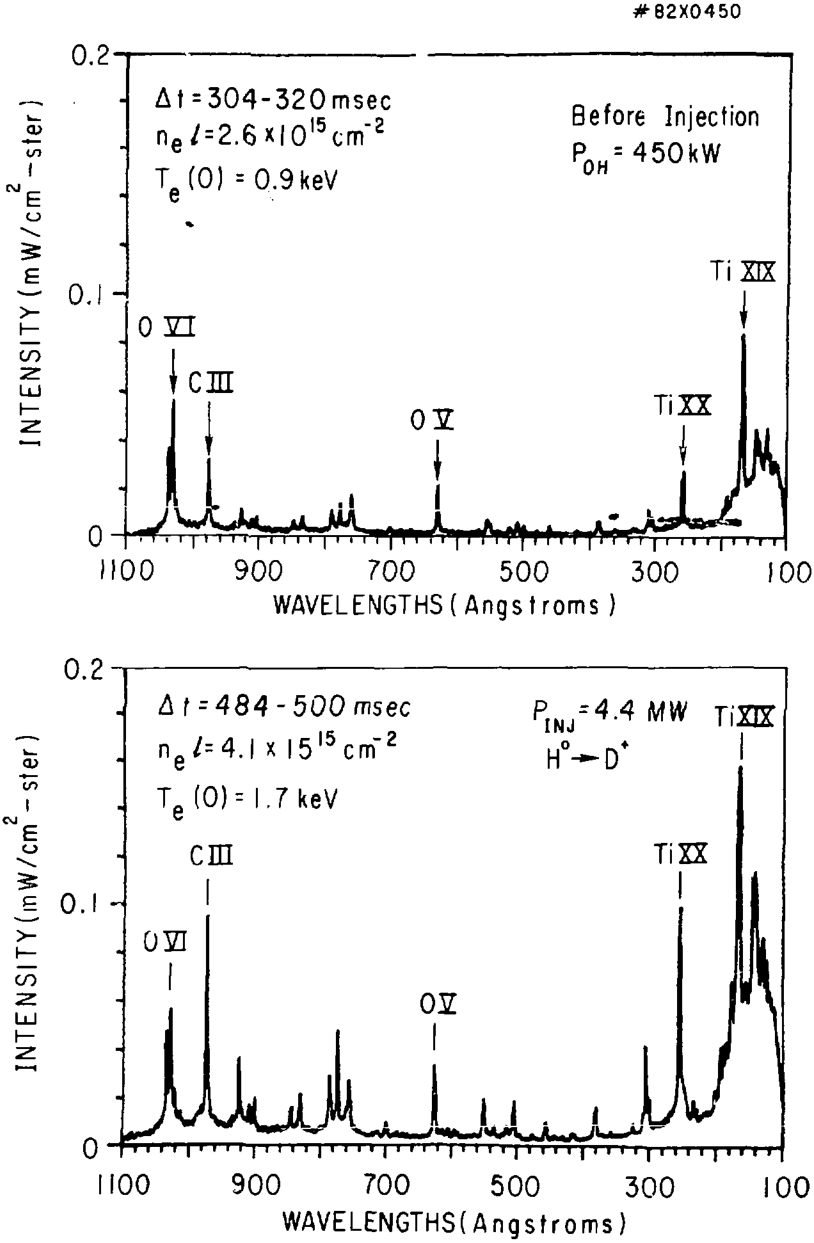

#82X0450
Δt = 304-320 msec
Before Injection
Ti XIX
O VI
C III
O V
Ti XX
INTENSITY (mW/cm2 - ster)
WAVELENGTHS (Angstroms)
Δt = 484 - 500 msec
Ti XIX
Ti XX
C III
O VI
O V
INTENSITY (mW/cm2 - ster)
WAVELENGTHS (Angstroms)

Fig. 6

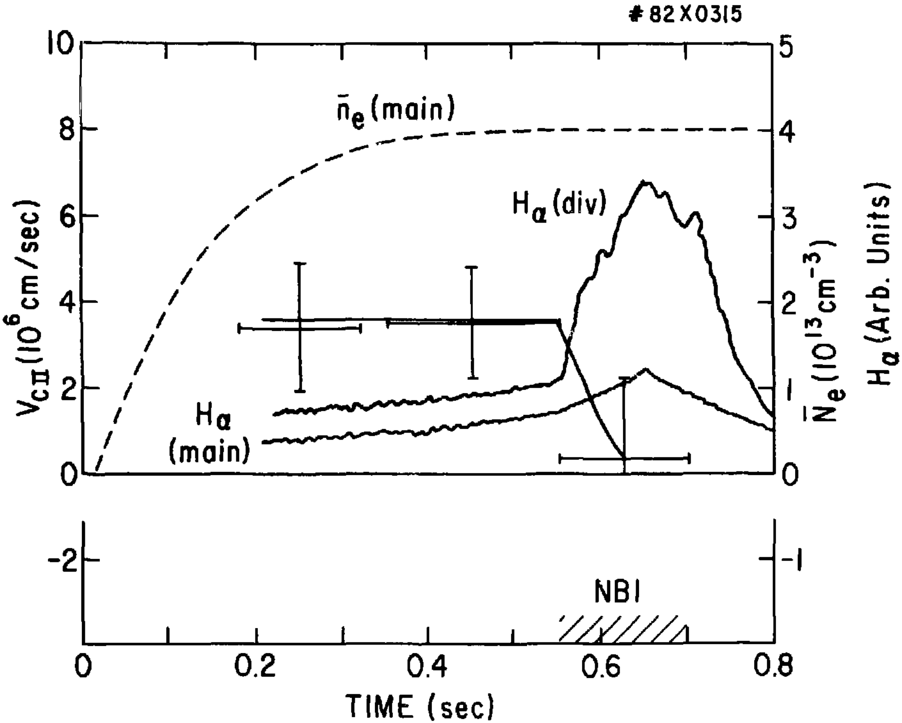

82X0315
$\bar{n}_e$(main)
H_α(div)
H_α (main)
NBI
$V_{CII}(10^6$cm/sec)
$\bar{N}_e(10^{13}$cm$^{-3})$
H_α(Arb. Units)
TIME (sec)
0
0.2
0.4
0.6
0.8
10
8
6
4
2
0
-2
5
4
3
2
1
0
-1

Fig. 7

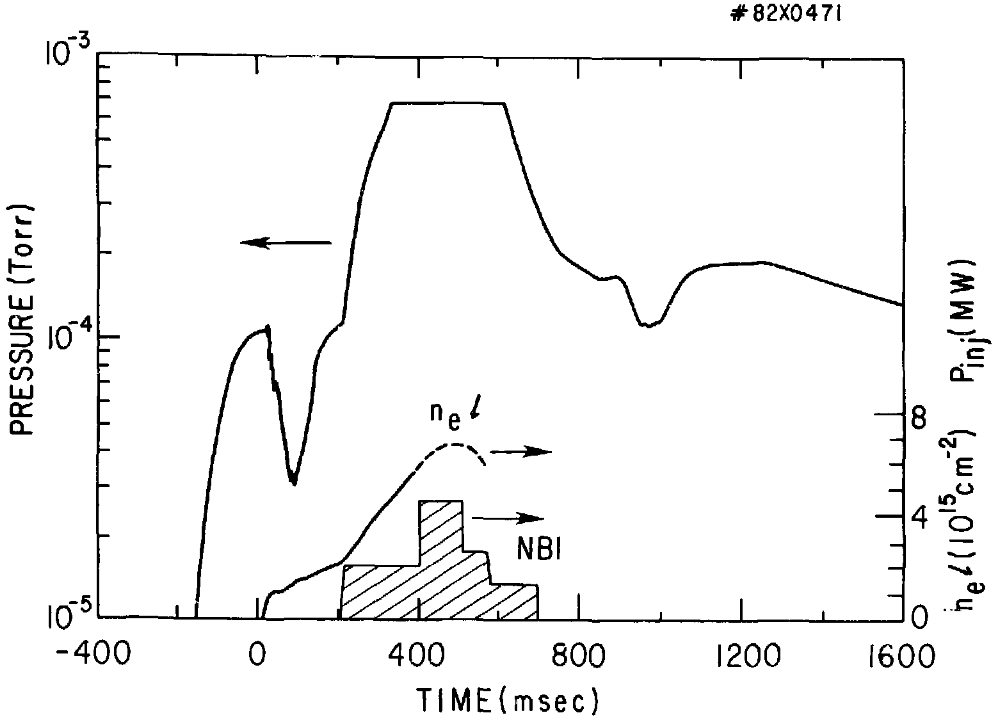
#82X0471
PRESSURE (Torr)
10^{-3}
10^{-4}
10^{-5}
-400
0
400
800
1200
1600
TIME (msec)
$n_e\ell$
NBI
0
4
8
$n_e\ell\,(10^{15}\,cm^{-2})$ P_{inj} (MW)

Fig. 8

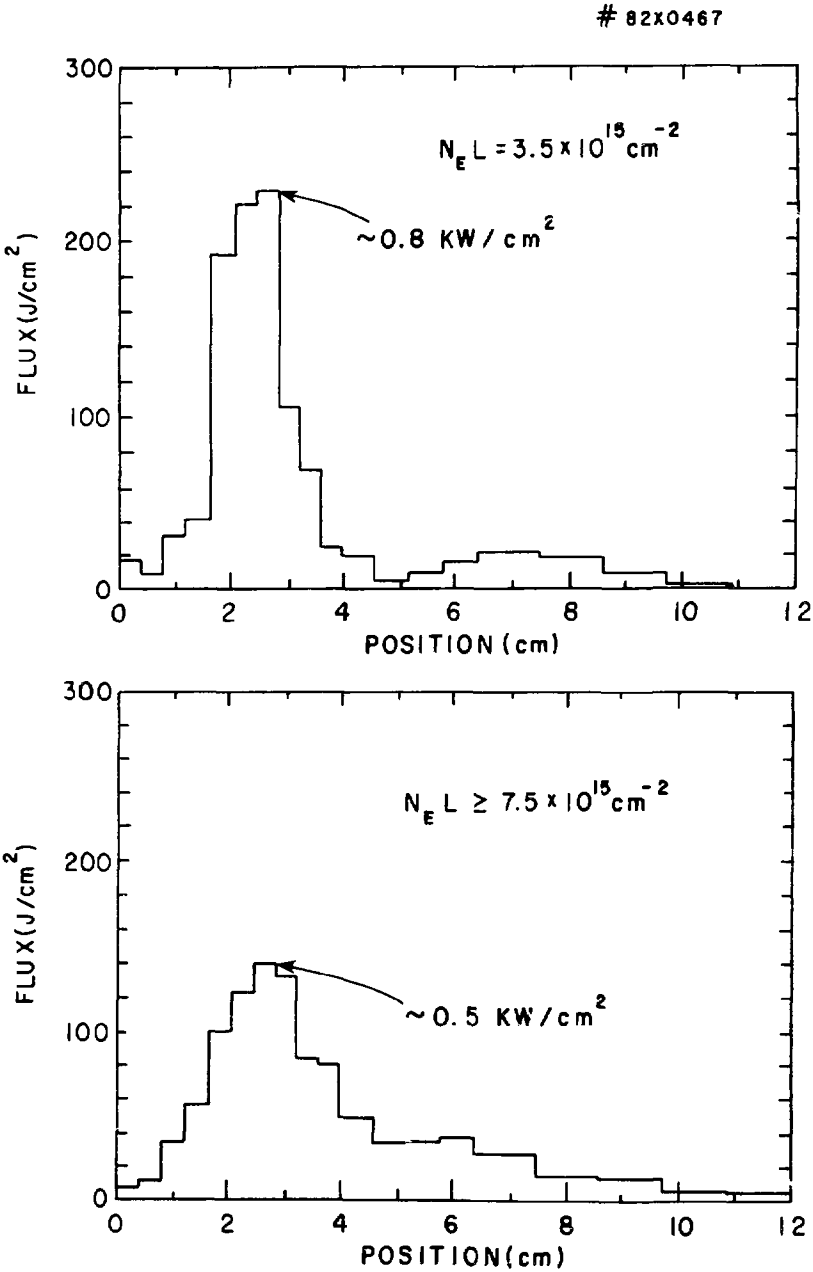

82X0467
300
200
100
0
FLUX(J/cm^2)
$N_E L = 3.5 \times 10^{15}$ cm^{-2}
~0.8 KW/cm^2
0 2 4 6 8 10 12
POSITION (cm)
$N_E L \geq 7.5 \times 10^{15}$ cm^{-2}
~0.5 KW/cm^2
POSITION(cm)

Fig. 9

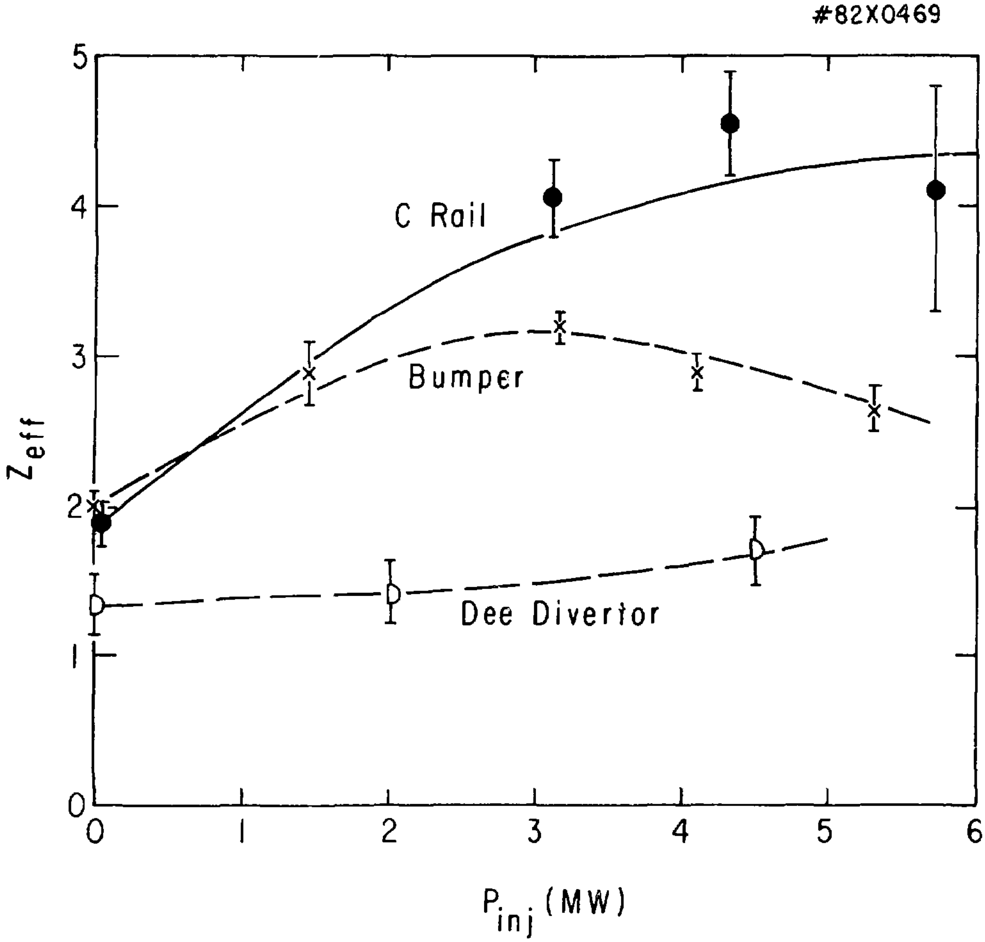

Fig. 10

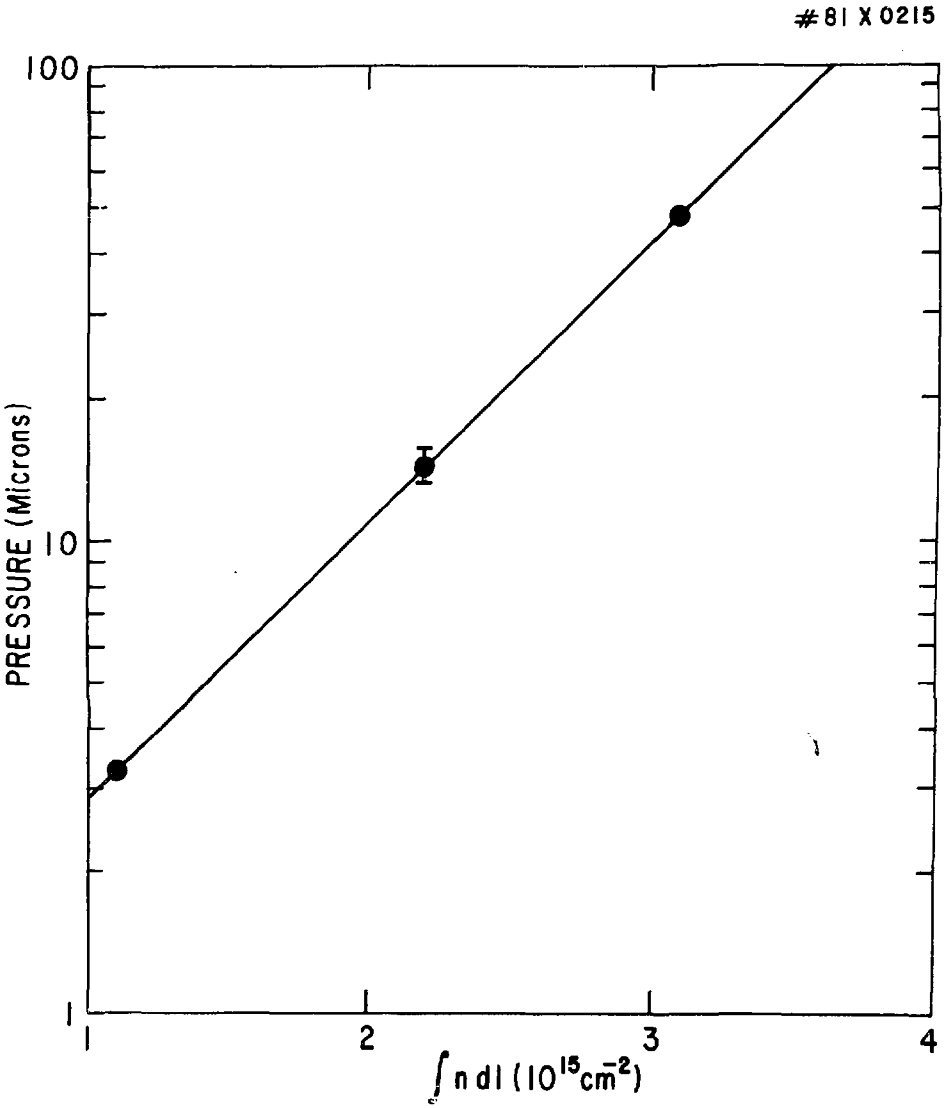

Fig. 11

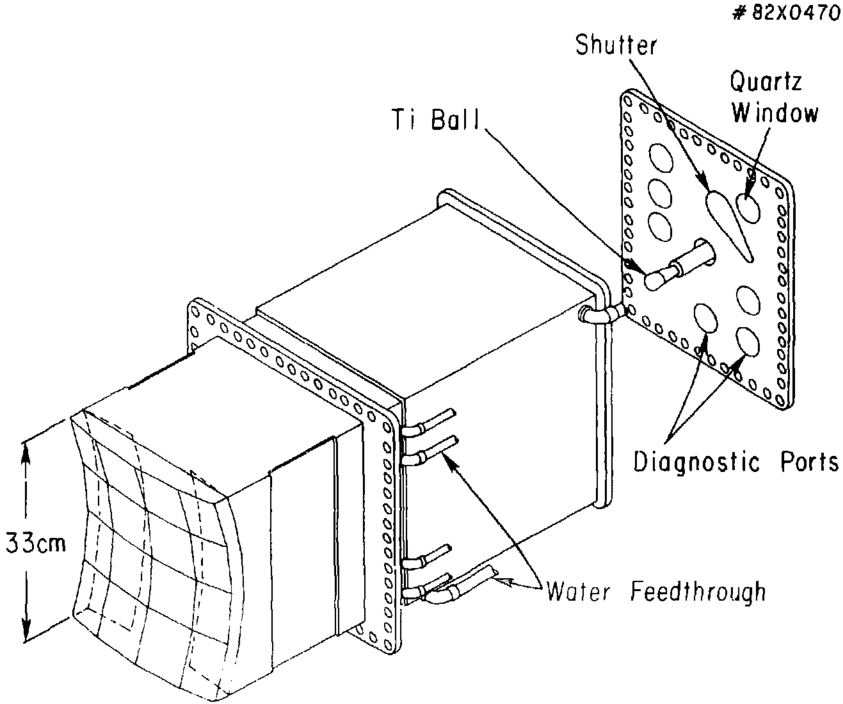
#82X0470
Shutter
Quartz
Window
Ti Ball
Diagnostic Ports
33cm
Water Feedthrough

Fig. 12a

#82X046B

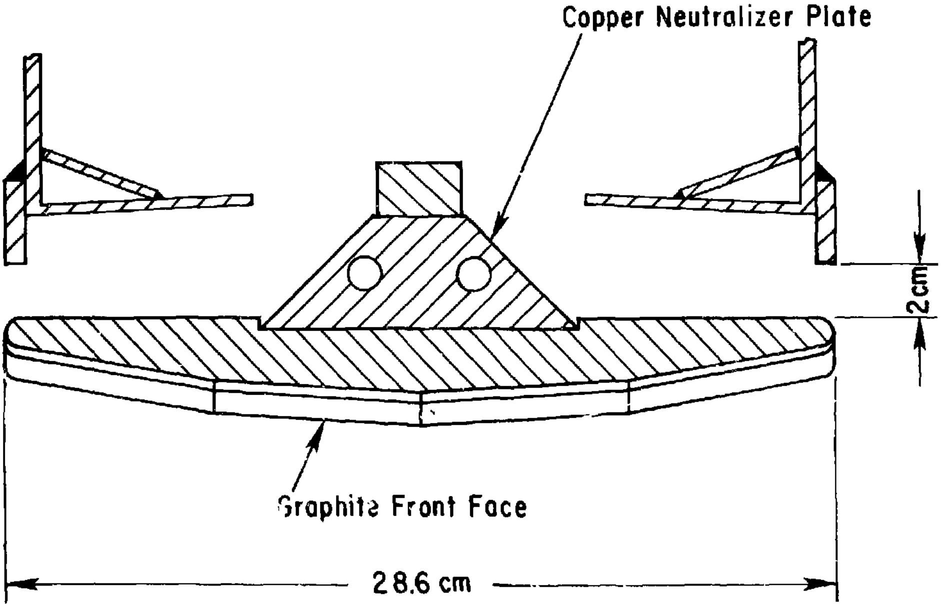

Fig. 12b

EXTERNAL DISTRIBUTION IN ADDITION TO TIC UC-20

Plasma Res Lab, Austra Nat'l Univ, AUSTRALIA
Dr. Frank J. Paoloni, Univ of Wollongong, AUSTRALIA
Prof. I.R. Jones, Flinders Univ., AUSTRALIA
Prof. M.H. Brennan, Univ Sydney, AUSTRALIA
Prof. F. Cap, Inst Theo Phys, AUSTRIA
Prof. Frank Verheest, Inst theoretische, BELGIUM
Dr. D. Palumbo, Dg XII Fusion Prog, BELGIUM
Ecole Royale Militaire, Lab de Phys Plasmas, BELGIUM
Dr. P.H. Sakanaka, Univ Estadual, BRAZIL
Dr. C.R. James, Univ of Alberta, CANADA
Prof. J. Teichmann, Univ of Montreal, CANADA
Dr. H.M. Skarsgard, Univ of Saskatchewan, CANADA
Prof. S.R. Sreenivasan, University of Calgary, CANADA
Prof. Tudor W. Johnston, INRS-Energie, CANADA
Dr. Hannes Barnard, Univ British Columbia, CANADA
Dr. M.P. Bachynski, MPB Technologies, Inc., CANADA
Zhengwu Li, SW Inst Physics, CHINA
Library, Tsing Hua University, CHINA
Librarian, Institute of Physics, CHINA
Inst Plasma Phys, SW Inst Physics, CHINA
Dr. Peter Lukac, Komenskeho Univ, CZECHOSLOVAKIA
The Librarian, Culham Laboratory, ENGLAND
Prof. Schatzman, Observatoire de Nice, FRANCE
J. Radet, CEN-BP6, FRANCE
AM Dupas Library, AM Dupas Library, FRANCE
Dr. Tom Mual, Academy Bibliographic, HONG KONG
Preprint Library, Cent Res Inst Phys, HUNGARY
Dr. R.K. Sundaram, Physical Research Lab, INDIA
Dr. S.K. Trehan, Panjab University, INDIA
Dr. Indra, Mohan Lal Das, Banaras Hindu Univ, INDIA
Dr. L.K. Chavda, South Gujarat Univ, INDIA
Dr. R.K. Chhajlani, Var Ruchi Marg, INDIA
B. Buti, Physical Research Lab, INDIA
Dr. Phillip Rosenau, Israel Inst Tech, ISRAEL
Prof. S. Cuperman, Tel Aviv University, ISRAEL
Prof. G. Rostagni, Univ Di Padova, ITALY
Librarian, Int'l Ctr Theo Phys, ITALY
Miss Clelia De Palo, Assoc EURATOM-CNEN, ITALY
Biblioteca, del CNR EURATOM, ITALY
Dr. H. Yamato, Toshiba Res & Dev, JAPAN
Prof. M. Yoshikawa, JAERI, Tokai Res Est, JAPAN
Prof. T. Uchida, University of Tokyo, JAPAN
Research Info Center, Nagoya University, JAPAN
Prof. Kyoji Nishikawa, Univ of Hiroshima, JAPAN
Sigeru Mori, JAERI, JAPAN
Library, Kyoto University, JAPAN
Prof. Ichiro Kawakami, Nihon Univ, JAPAN
Prof. Satoshi Itoh, Kyushu University, JAPAN
Tech Info Division, Korea Atomic Energy, KOREA
Dr. R. England, Civdad Universitaria, MEXICO
Bibliotheek, Fom-Inst Voor Plasma, NETHERLANDS
Prof. B.S. Liley, University of Waikato, NEW ZEALAND
Dr. Suresh C. Sharma, Univ of Calabar, NIGERIA
Prof. J.A.C. Cabral, Inst Superior Tech, PORTUGAL
Dr. Octavian Petrus, ALI CUZA University, ROMANIA
Dr. R. Jones, Nat'l Univ Singapore, SINGAPORE
Prof. M.A. Hellberg, University of Natal, SO AFRICA
Dr. Johan de Villiers, Atomic Energy Bd, SO AFRICA
Dr. J.A. Tagle, JEN, SPAIN
Prof. Hans Wilhelmson, Chalmers Univ Tech, SWEDEN
Dr. Lennart Stenflo, University of UMEA, SWEDEN
Library, Royal Inst Tech, SWEDEN
Dr. Erik T. Karlson, Uppsala Universitet, SWEDEN
Centre de Recherchesen, Ecole Polytech Fed, SWITZERLAND
Dr. W.L. Weise, Nat'l Bur Stand, USA
Dr. W.M. Stacey, Georg Inst Tech, USA
Dr. S.T. Wu, Univ Alabama, USA
Mr. Norman L. Oleson, Univ S Florida, USA
Dr. Benjamin Ma, Iowa State Univ, USA
Magne Kristiansen, Texas Tech Univ, USA
Dr. Raymond Askew, Auburn Univ, USA
Dr. V.T. Tolok, Kharkov Phys Tech Ins, USSR
Dr. D.D. Ryutov, Siberian Acad Sci, USSR
Dr. M.S. Rabinovich, Lebedev Physical Inst, USSR
Dr. G.A. Eliseev, Kurchatov Institute, USSR
Dr. V.A. Glukhikh, Inst Electro-Physical, USSR
Prof. T.J. Boyd, Univ College N Wales, WALES
Dr. K. Schindler, Ruhr Universitat, W. GERMANY
Nuclear Res Estab, Julich Ltd, W. GERMANY
Librarian, Max-Planck Institut, W. GERMANY
Dr. H.J. Kaeppler, University Stuttgart, W. GERMANY
Bibliothek, Inst Plasmaforschung, W. GERMANY